New microscopic pushbroom hyperspectral imaging system for application in diabetic retinopathy research

Qingli Li
East China Normal University
Information Science
No. 500, Dongchuan Rd.
Shanghai, 200241 China

Yongqi Xue
Gonghai Xiao
Shanghai Institute of Technical Physics
Shanghai, China

Jingfa Zhang
Shanghai Jiaotong University
School of Medicine
Laboratory of Clinical Visual Science
Shanghai, China

Abstract. To aid ophthalmologists in determining the pathogenesis of diabetic retinopathy and in evaluating the effects of medication, a microscopic pushbroom hyperspectral imaging system is developed. 40 healthy Wistar rats of half gender are selected in this study. They are divided into three groups (six rats failed to be models). 10 normal rats as the normal control group, 12 diabetic rats without any treatment as the model control group, and another 12 diabetic rats treated with LCVS1001 as the LCVS1001 group. The microscopic hyperspectral image of each retina section is collected and processed. Some typical spectrum curves between 400 and 800 nm of the outer nuclear layer are extracted, and images at various wavelengths are analyzed. The results show that a small trough appears near 522.2 nm in the typical spectrum curve of the model control group, and the transmittance of it is higher than that of the normal control group. In addition, the spectrum of the LCVS1001 group changes gradually to the normal spectrum after treatment with LCVS1001. Our findings indicate that LCVS1001 has some therapeutic effect on the diabetic retinopathy of rats, and the microscopic pushbroom hyperspectral imaging system can be used to study the pathogenesis of diabetic retinopathy.
[DOI: 10.1117/1.2821210]

Keywords: diabetic retinopathy; outer nuclear layer; microscopic hyperspectral imaging; spectrum.

Paper 07127R received Apr. 5, 2007; revised manuscript received Jul. 13, 2007; accepted for publication Jul. 17, 2007; published online Dec. 7, 2007.

1 Introduction

Diabetic retinopathy is a microvascular complication that can occur in diabetic patients. The occurrence of diabetic retinopathy results in the disturbance of visual capability, and can eventually lead to blindness. The longer a person has untreated diabetes, the higher the chance of developing diabetic retinopathy.[1,2] It is very important for ophthalmologist to thoroughly understand the pathogenesis of diabetic retinopathy, so that the disease can be treated successfully and the worse case can be anticipated.[3,4] One way to study this disease is employing an optical microscope to observe retina sections.[5–7] However, this method can only receive qualitative analysis results, and it is difficult to find the relationship between the pathological changes and the biochemical mechanism leading to these changes.

In this work, a microscopic pushbroom hyperspectral imaging (MPHI) system was developed to observe retina sections of normal, diabetic, and treated diabetic rats. The microscopic hyperspectral image data of each group were collected and processed. Typical spectrum curves of the outer nuclear layer of each group were extracted, and images at various wavelengths were analyzed. The temporary results of our current progress show that the MPHI system is helpful for the study of diabetic retinopathy.

2 Materials and Methods

2.1 *Animals*

A total of 40 healthy Wistar rats (provided by the Laboratory of Clinical Visual Science, Shanghai Jiaotong University, China) aged 7 weeks old of half gender were selected for this study. Animals were acclimated to the laboratory environment for 5 to 7 days before entering the study. While in the home cage environment, the animals were allowed free access to water and were maintained on a commercial rat diet under standard laboratory conditions. Ten rats were selected as the normal control group and fed with ordinary diet. 30 overnight fasted rats were injected with streptozocin (60 mg/kg dissolved in 3-mM citrate buffer pH 4.5) intraperitoneally.[8] After ten days (six rats failed to be models) 24 rats showed plasma glucose level >300 mg/dl. They were classified as diabetic and were included in the study. After six weeks, diabetic retinopathy developed in these rats. They were divided randomly into a model control group and LCVS1001 group with 12 in each. The LCVS1001 group was treated with LCVS1001 (provided by the Laboratory of Clinical Visual Science of Shanghai Jiaotong University, China) once daily for five

Address all correspondence to: Dr. Qingli Li, East China Normal University, Information Science, No. 500, Dongchuan Rd., Shanghai, 200241 China. E-mail: qlli@cs.ecnu.edu.cn

1083-3668/2007/12(6)/064011/4/$25.00 © 2007 SPIE

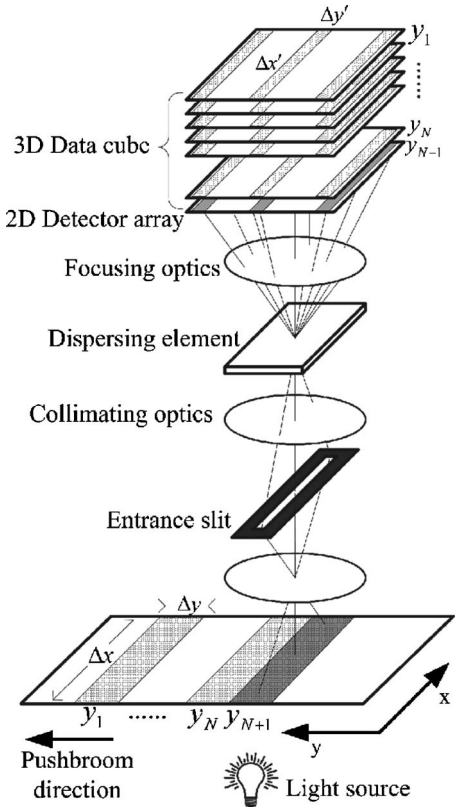

Fig. 1 Schematic diagram of MPHI.

weeks. LCVS1001 is a glycoprotein that has demonstrated protective functions for vascular and neuronal cells, and has some therapeutic effect on early diabetic retinopathy. At last, the rats were divided into three groups: 10 normal rats as the normal control group (N), 12 diabetic rats without any treatment as the model control group (M), and another 12 diabetic rats treated with LCVS1001 as the LCVS1001 group (L).

2.2 *Microscopic Pushbroom Hyperspectral Imaging System*

The microscopic pushbroom hyperspectral imaging (MPHI) system is designed based on the principle of a pushbroom hyperspectral imager commonly used in remote sensing.[9,10] It includes a microscope, a spectrometer, a charge-coupled device (CCD) detector, a parallel moving device, and a data collection and control module. As shown in Fig. 1, the sample stripe of a retina section is first imaged on the entrance slit, and then dispersed vertically by the grating and prism module, and imaged on the CCD detector at last. If we define the dimension that is parallel to the slit as the spatial dimension, and the dimension that is vertical to the silt as the spectrum dimension, then each photoconductive element of the spatial dimension can have an image of a certain band of the sample stripe. So each image of the CCD detector corresponds to a hyperspectral image of the sample stripe. To achieve the whole microscopic hyperspectral image of a sample, the system needs a pushbroom in another spatial dimension. In aviation remote sensing, the frontal movement of the plane carries out the pushbroom procedure. However, in the MPHI system, a parallel moving device is used to realize the pushbroom procedure. The microscope stage is fixed on the parallel moving device driven by a step motor. The step motor is controlled by a single chip microcomputer. So a tissue section on the objective table can be scanned automatically under the control of the microcomputer. Then a hypersectral imagery data cube of the section can be acquired after the pushbroom procedure.

The MPHI system captures image scenes in contiguous but narrow spectral bands over the visible wavelength range of the electromagnetic spectrum. In this way, it can potentially capture hundreds of spectral bands covering the narrow spectral features of the captured material as close as possible. The image data provided by the MPHI system can be visualized as a 3-D cube or a stack of multiple 2-D images (Fig. 2), because of its intrinsic structure, where the cube face is a function of the spatial coordinates $f(x,y)$ and the depth is a function of wavelength. In this case, each spatial point on the face is characterized by its own spectrum (often called the spectral signature). This spectrum directly corresponds to the amount of energy that the retina section represented, as hyperspectral sensors commonly utilize the simple fact that an organism emits light in certain frequency bands. Consequently, the microscopic hyperspectral data provide a wealth of information about an image scene that is potentially very helpful in determining the pathogenesis and evaluating the effects of medication.

2.3 *Methods for Observing of Retina*

Hyperspectral imaging was performed on retinas at the end of 13 weeks. All rats were sacrificed with deep anesthesia. For cryostat section sample preparation, the eyes were fixed in phosphate buffered saline (PBS)-buffered 4% paraformaldehyde for 24 h, and then were opened along the ora serrata. The posterior eyecups were dehydrated through a gradient

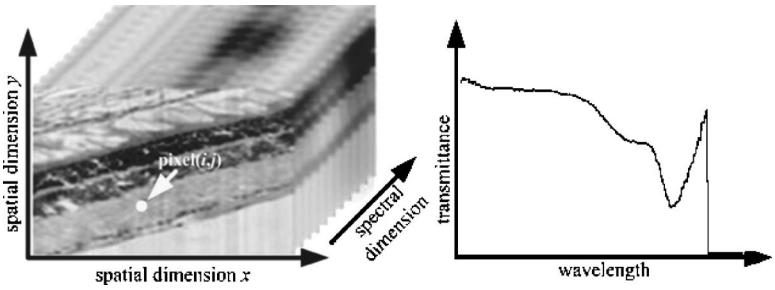

Fig. 2 The microscopic hyperspectral imagery data cube and the spectrum of pixel (i,j).

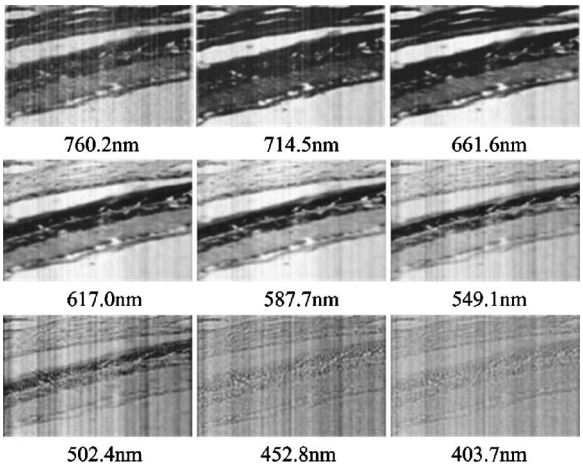

Fig. 3 Images of normal retina sections collected at various wavelengths using the MPHI system.

concentration of sucrose from 10 to 30%. Following dehydration, the eyecups were embedded in optimal cutting temperature (OCT) compound (Tissue Tek, Sakura, Japan) for sectioning. Serial sections that passed through the optic nerve head were analyzed. In this experiment, 10-μm-thick sections were used. Each retina section was stained with hematoxylin and scanned by the MPHI system.

3 Results

3.1 *Images Collected at Various Wavelengths*

Figure 3 illustrates a representative subtotal of spectral images of a normal retina section captured at various wavelengths using the MPHI system. The microscopic hyperspectral data consist of 460×300 pixels with 240 spectral bands ranging from the wavelength $\lambda 1$ (403.7 nm) to $\lambda 240$ (865.2 nm) with about 2-nm spectral resolutions. From Fig. 3, it can be seen that there are many differences among the outer nuclear layer, inner nuclear layer, and the inner plexiform layer in different band images.

3.2 *Spectral Signatures of Diabetic Retina*

According to the electromagnetic theory, tissues emit different amounts of energy at different wavelengths of the electromagnetic spectrum. Spectral characteristics in different wavelength regions yield a distinguishable spectral signature, making diabetic retinopathy distinguishable. Figure 4 shows the relative transmittance spectrum curves of the outer nuclear layer of each group as a function of spectral bands (wavelength). The transmittance difference between the normal and diabetic is large in the spectral range of 636 to 722 nm. The diabetic spectrum has a small trough near the wavelength 522.2 nm. To describe the spectral characteristics quantitatively, we introduced the definition of a spectral absorption index (SAI) from remote sensing.[11] We select three samples randomly from each group and calculate the spectral absorption index (Table 1). Table 1 shows that there are certain differences among three groups in SAI, and the LCVS1001 group changes gradually to the normal control group. The results also show that the MPHI system has better sensitivity and specificity in diabetic retinopathy research and diagnosis.

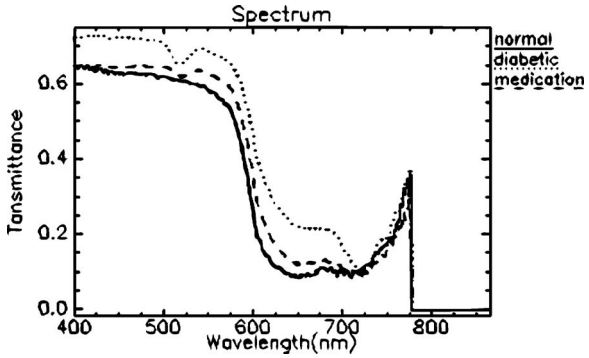

Fig. 4 Typical spectrum of outer nuclear layer of N, M, and L retina sections.

3.3 *Pathological Change Detection*

According to the remote sensing theory, if things are irradiated by an electromagnetic wave, electronic transition, atomic oscillation, and molecular rotation will take place. So almost all things in the nature have some spectral characters at certain wavelengths that can imply their biochemical information. These spectral characters can be used to analyze components of things and detect their biochemical changes. As for biological tissues, biochemical or pathological changes can be detected by analyzing the difference between spectrums. In this experiment, the biochemical changes of diabetic retinas can be detected easily by applying the spectral angle mapper (SAM) algorithm,[12] as normal and abnormal cells have different characters in the spectrum. Figure 5 shows the detecting result with SA=0.1. As a preliminary experiment, we only get the specific areas where there is a spectral difference between diabetic and nondiabetic. Further research is needed in the future to understand what the meaning of different spectra is and why the spectra changes.

4 Discussion

Current ophthalmic hyperspectral imaging systems are mainly used in imaging retinas macroscopically.[13,14] One of the ad-

Table 1 SAI of outer nuclear layer from N, M, and L.

Group	Sample	ρ_{s1}	ρ_M	ρ_{s2}	*SAI*
Normal control	N1	0.322	0.085	0.549	5.22
	N2	0.332	0.076	0.53	5.76
	N3	0.351	0.082	0.546	5.56
Model control	M1	0.371	0.224	0.662	2.35
	M2	0.38	0.217	0.659	2.44
	M3	0.376	0.221	0.67	2.42
LCVS1001	L1	0.315	0.133	0.633	3.65
	L2	0.32	0.125	0.623	3.86
	L3	0.346	0.112	0.59	4.25

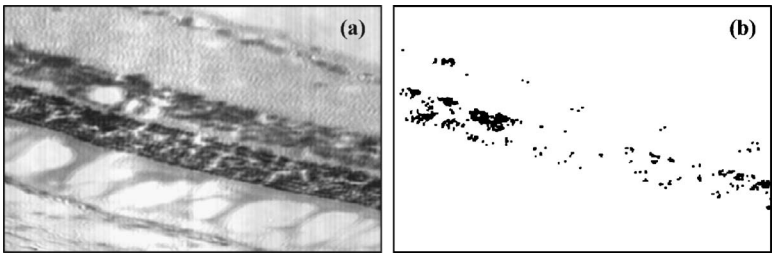

Fig. 5 Detection of pathological changes: (a) 587.7-nm band image of retina section of diabetic rats, and (b) localization of pathological changes.

vantages is that these systems can provide the hyperspectral image of the whole retina *in vivo* and diagnose some retinal disease.[15] However, these systems cannot provide microscopic hyperspectral images of each retinal layer or study the retinal disease microscopically. In this work, a home-built microscopic pushbroom hyperspectral imaging (MPHI) system has been developed and some microscopic hyperspectral images of retina sections of rats have been acquired. Because the microscopic hyperspectral data can provide both spatial characters and spectral signatures of retina sections, the information can potentially serve in the identification of pathological changes based on particular biochemical and structural features. Also, imaging spectral bands that correspond to the maximum differentiation between the spectral characteristics of normal and abnormal retina will result in maximization of the perceived contrast. This will enable better localization of the pathological changes, and will improve the accuracy in the determination of cluster borders, which is very important in treatment evaluation and planning. Our initial observations show that the MPHI system contributes to the development of novel diagnostic methods and systems, while also opening new directions that need to be explored.

It should be noted that our study is a preliminary report and has several important limitations. Histological changes in the outer nuclear layer of retinas were only assessed on a gross level and not analyzed by objective histopathologic methods. Spectra of other retinal layers were not extracted and analyzed. More detailed studies examining diabetes-induced pathological changes in the whole retina are in the works.

Acknowledgments

We are grateful for the expert medical assistance provided by G.T. Xu from the Laboratory of Clinical Visual Science, Shanghai Jiaotong University, China.

References

1. S. Fransen, T. Leonard-Martin, W. Feuer, and P. Lloyd Hildebrand, "Clinical evaluation of patients with diabetic retinopathy," *Ophthalmology* **109**, 595–601 (2002).
2. J. P. Glover, J. L. Jacot, and M. D. Basso, "Retinal capillary dilation: early diabetic-like retinopathy in the galactose-fed rat model," *J. Ocul. Pharmacol. Ther.* **16**, 167–172 (2000).
3. H. Hans-Peter, K. Irmtraud, and W. Susanna, "Islet transplantation inhibits diabetic retinopathy in the sucrose-fed diabetic cohen rat," *Invest. Ophthalmol. Visual Sci.* **34**, 2092–2096 (1993).
4. R. Klein, B. Klein, S. Moss, T. Wong, L. Hubbard, K. Cruickshanks, and M. Palta, "Retinal vascular abnormalities in persons with type 1 diabetes: The Wisconsin Epidemiologic Study of Diabetic Retinopathy: XVIII," *Ophthalmology* **110**, 2118–2125 (2003).
5. L. Jonathan, D. Matthew, K. Hockmann, and K. B. Alexander, "Effects of acute delivery of endothelin-1 on retinal ganglion cell loss in the rat," *Exp. Eye Res.* **82**, 132–145 (2006).
6. P. Niall, M. A. Tariq, M. Thomas, J. D. Ian, D. Baljean, H. E. Robert, Y. Kanagasingam, and J. C. Ian, "Retinal image analysis: concepts, applications and potential," *Prog. Retin Eye Res.* **25**, 99–127 (2006).
7. Y. L. Zhu, K. O. Kevin, K. M. Belinda, S. P. Tae, and M. G. Jeffrey, "Constitutive nitric oxide synthase activity is required to trigger ischemic tolerance in mouse retina," *Exp. Eye Res.* **82**, 153–163 (2006).
8. E. M. Halim and H. Ali, "Reversal of diabetic retinopathy in streptozotocin induced diabetic rats using traditional Indian anti-diabetic plant, azadirachta indica (L.)," *Indian J. Clin. Biochem.* **17**, 115–123 (2002).
9. H. B. Li, R. Shu, and Y. Q. Xue, "Pushbroom hyperspectral imager and its potential application to ocenographic remote sensing," *Int. J. Infrared Millim. Waves* **21**, 429–433 (2002).
10. G. H. Xiao, R. Shu, and Y. Q. Xue, "Design of microscopic hyperspectral imaging system," *Opt. Precision Eng.* **12**, 367–372 (2004).
11. Y. N. Wang, L. F. Zheng, and Q. X. Tong, "The spectral absorption identification model and mineral mapping by imaging spectrometer data," *Remote Sens. Environ.* **11**, 20–31 (1996).
12. F. A. Kruse, A. B. Lefkoff, and J. W. Boardman, "The spectral image processing system (SIPS)-software for integrated analysis of AVIRIS data," *Sum. 4th Ann. JPL Airborne Geosci. Workshop*, pp. 23–25, JPL Pub. (1992).
13. C. David, A. Mark, B. Gregory, and S. G. Warren, "Use of spectral imaging for the diagnosis of retinal disease," *Conf. Proc. Lasers Electro-Opt. Soc. Ann. Mtg. LEOS* **1**, 220–221 (1999).
14. J. M. Beach, K. J. Schwenzer, and S. Srinivas, "Oximetry of retinal vessels by dual-wavelength imaging: calibration and influence of pigmentation," *J. Appl. Physiol.* **86**, 748–758 (1999).
15. R. J. William, W. W. Daniel, F. Wolfgang, H. Mark, and B. Greg, "Snapshot hyperspectral imaging in ophthalmology," *J. Biomed. Opt.* **12**, 014036 (2007).